

# Half metallic digital ferromagnetic heterostructure composed of a $\delta$ -doped layer of Mn in Si

M. C. Qian,<sup>1</sup> C. Y. Fong,<sup>1</sup> Kai Liu,<sup>1</sup> Warren E. Pickett,<sup>1</sup> J. E. Pask,<sup>2</sup> and L. H. Yang<sup>2</sup>

<sup>1</sup>*Department of Physics, University of California, Davis CA 95616-8677*

<sup>2</sup>*Lawrence Livermore National Laboratory,  
University of California, Livermore, CA 94551*

(Dated: May 1, 2018)

## Abstract

We propose and investigate the properties of a digital ferromagnetic heterostructure (DFH) consisting of a  $\delta$ -doped layer of Mn in Si, using *ab initio* electronic-structure methods. We find that (i) ferromagnetic order of the Mn layer is energetically favorable relative to antiferromagnetic, and (ii) the heterostructure is a two-dimensional half metallic system. The metallic behavior is contributed by three majority-spin bands originating from hybridized Mn-*d* and nearest-neighbor Si-*p* states, and the corresponding carriers are responsible for the ferromagnetic order in the Mn layer. The minority-spin channel has a calculated semiconducting gap of 0.25 eV. Analysis of the total and partial densities of states, band structure, Fermi surfaces and associated charge density reveals the marked two-dimensional nature of the half metallicity. The band lineup is found to be favorable for retaining the half metal character to near the Curie temperature ( $T_C$ ). Being Si based and possibly having a high  $T_C$  as suggested by an experiment on dilutely doped Mn in Si, the heterostructure may be of special interest for integration into mature Si technologies for spintronic applications.

PACS numbers: 75.50.Pp, 71.15.Mb, 71.70.Gm, 72.80.Cw

Doping magnetic transition metal elements into semiconductors has attracted much attention recently, especially the doping of Mn in GaAs[1], which has inspired much interest in the new and immensely promising field of spintronics [2, 3, 4]. Since 2000, a new class of potential spintronic materials has been discovered: the half metallic transition metal pnictides with zincblende structure. Two such compounds, CrAs[5] and CrSb[6], have been grown in thin film form. Many other pnictides and carbides[7, 8, 9] have been predicted based on first-principles calculations in the generalized gradient approximation (GGA)[10]. Related quantum structures, such as superlattices[11, 12, 13] and quantum dots[14], have also been studied. Sanvito and Hill[15] investigated the half metallic properties of a digital ferromagnetic heterostructure (DFH) composed of a layer of Mn in GaAs. The key property of all such half metallic materials is the 100 % spin polarization at the Fermi energy,  $E_F$ . Therefore, the magnetoresistance (MR) effect is expected to be much larger and becomes infinite in the ideal case. Devices made of these materials, such as MR sensors, memories and switches, will have superior qualities to the ones presently available. However, the realization of devices based on these materials has been hindered by difficulties in growth and fabrication processes involving III-V compounds. Fabrication techniques for Si based devices are more mature; and so they might be more readily manufactured, if corresponding half metallic devices could be engineered. The prediction of ferromagnetic order in Mn-doped bulk Si[16] and the growth of dilutely doped Mn in Si[17, 18] have been reported. The experimental results are particularly encouraging because the measured Curie temperature,  $T_C$ , is over 400 K, in stark contrast to Mn-doped GaAs which suffers from a  $T_C$  far below room temperature. A critical shortcoming of Mn-doped GaAs with respect to spintronic applications might thus be surmounted by such Si based materials.

Here, we report our design of a DFH consisting of a  $\delta$ -doped layer of Mn in a Si substrate (Mn/Si-DFH), with a  $\delta$  function (single layer) doping profile along the growth direction, and our prediction that this DFH is a two-dimensional half metal. We find that the metallic properties are contributed by extended states originating from hybridized Mn- $d$  and nearest-neighbor Si- $p$  majority-spin states, while the minority-spin channel is semiconducting with a 0.25 eV gap.

We employed planewave pseudopotential density-functional methods[19], in the generalized gradient approximation (GGA) to exchange and correlation[10]. Ultra-soft pseudopotentials[20] were used to facilitate the accurate treatment of transition metal atoms.

The heterostructure was modeled by a unit cell consisting of 32 atoms in layers along the [001]-direction of epitaxial growth, as shown in Fig. 1. The unit cell is tetragonal with  $\mathbf{a}$  and  $\mathbf{b}$  axes along the [110]- and  $[\bar{1}10]$ -directions, and lattice constant  $a_0/\sqrt{2}$ , where  $a_0 = 5.45$  Å is the optimized lattice constant of Si crystal. The indices are defined with respect to the conventional cell. We have checked the effect of the thickness of the Si region from 15 to 39 Si layers along the [001]-direction. The half metallic properties and the density states of the majority-spin at  $E_F$  remain unaffected. The gap between the lowest unoccupied state in the minority-spin channel and  $E_F$  is 0.15 eV at 15 Si layers separation and stabilized to 0.16 eV at separations of 31 Si layers or more. Further details will be presented elsewhere[21]. The separation between Mn layers in neighboring cells was sufficient to make cell-cell interactions negligible, as we discuss below. A planewave cutoff of 450 eV and Monkhorst-Pack[22] mesh of  $11 \times 11 \times 1$   $\mathbf{k}$ -points was used in all calculations. Larger  $\mathbf{k}$ -point sets were employed to verify convergence of the above set to the order of 1 meV/atom. Wigner-Seitz sphere radii of 1.35 Å and 1.32 Å were used for Mn and Si atoms, respectively, to construct projected densities of states. Atomic positions were optimized by conjugate-gradient minimization of the total energy.

The magnetic moment per unit cell, density of states at the Fermi energy, and energy difference between ferromagnetic and antiferromagnetic ordering for the unrelaxed and relaxed cases are given in Table 1. Without lattice relaxation, the magnetic moment is an integer,  $3.0 \mu_B$ . There is a gap of 0.20 eV in the minority-spin states. The effect of lattice relaxation is small because the optimized lattice constant of Si (5.45 Å) is close to that of (hypothetical) zincblende MnSi (5.48 Å)[21]. The gap for the relaxed case opens slightly to 0.25 eV. Both with and without relaxation, the ferromagnetic phase has lower energy than the antiferromagnetic phase. Since the relaxation effect will not alter our conclusions about DFH, in the following, we focus our analysis on the unrelaxed case.

The total and partial densities of states (PDOS) for the majority- and minority-spin channels are shown in Fig. 2. The PDOSs show projections onto the Mn, nearest Si (Si(I)), and farthest Si (Si(II)) atoms. Considering first the majority-spin states, we find a finite density of states at  $E_F$ , as shown in the top panel. The states in a 3 eV range around  $E_F$  (from  $\sim -1$  to  $+2$  eV) show strong hybridization between Mn- $t_{2g}$  and Si(I)- $p$  states (second and third panels). In contrast, there is no significant contribution from the more distant Si(II) atoms. The bonding states centered  $\sim 2.6$  eV below  $E_F$  exhibit correspondingly

TABLE I: Comparison of the unrelaxed and relaxed cases for Mn  $\delta$ -doped in Si. The magnetic moment  $m$ , density of states at the Fermi energy  $N(E_F)$  per eV-unit cell, ferromagnetic–antiferromagnetic energy difference  $E_{FA}$ , and minority-state gap  $E_g$  are listed. The difference  $E_{FA} = E_{FM} - E_{AFM}$  between FM and AFM ordering is calculated for the unit cell with one Mn-Mn pair. For both cases, the FM ordering has lower energy.

	$m(\mu_B)$	$N(E_F)$	$E_{FA}(\text{meV})$	$E_g(\text{eV})$
Unrelaxed	3.0	1.06	-523.91	0.20
Relaxed	3.0	1.25	-442.38	0.25

strong Mn- $t_{2g}$ -Si(I)- $p$  character. The nonbonding Mn- $e_g$  states are located  $\sim 2.5$  eV below  $E_F$ , concentrated in a somewhat narrower range of about 1 eV. The conduction states  $\sim 2$  eV above  $E_F$  and higher are contributed mainly by the Si atoms. Considering now the minority-spin channel, we find a semiconducting gap of  $\sim 0.20$  eV between valence and conduction bands. The valence states are mainly bulk Si, with one band of Mn- $t_{2g}$ -Si(I)- $p$  character at  $\sim 1$  eV below  $E_F$ . The conduction states originate from both antibonding  $p$ - $t_{2g}$  hybrid states and nonbonding  $e_g$  states of the Mn, leading to a peak at  $\sim 0.5$  eV. The more distant Si(II) atoms contribute a broad manifold extending to 4 eV below  $E_F$ , much as in Si crystal. The results indicate that the interaction of the Mn atom is confined primarily to its nearest-neighbor Si(I) atoms.

The band structure along symmetry lines in the  $\mathbf{k}_x$ - $\mathbf{k}_y$  plane ( $\Gamma$ -R-X- $\Gamma$ ) and along the  $\mathbf{k}_z$ -direction ( $\Gamma$ -Z) in the energy range  $-1.5$  to  $1.5$  eV is shown in Fig. 3. The sizes of the circles indicate the contribution from Mn- $d$  states: larger circles indicate larger contributions. In Fig. 3(a), three majority-spin bands pass through the Fermi energy in the  $\mathbf{k}_x$ - $\mathbf{k}_y$  plane. We label these bands 1, 2 and 3. The lowest energy states of the three bands are at the R point and are occupied. Around the  $\Gamma$  point, the three bands are unoccupied. As discussed above in PDOS, the states in the vicinity of  $E_F$  contributing to the conduction originate from the hybridization of Mn- $t_{2g}$  and (near-neighbor) Si(I)- $p$  states. Along  $\Gamma$ -Z, the marked flatness of the associated bands indicates the negligible interaction between Mn planes: the states are extended along the planes and well localized perpendicular to them, forming a metallic two dimensional sheet of majority carriers only. Compared to the corresponding bands along  $\Gamma$ -X of the Mn/GaAs DFH studied by Sanvito and Hill [15], the partially filled

bands in Mn/Si-DFH are substantially broader, reflecting the more ionic character of the As atoms relative to Si. In Fig. 3(b), the band structure for the minority-spin channel is shown. The semiconducting gap is indirect with the top of the valence band near the  $\Gamma$  point and the bottom of the conduction band at the zone corner R point. From the above, then, it is clear that the carriers in the Mn/Si-DFH come from three majority-spin bands, and mediate the exchange interactions between the local magnetic moments which give rise to the ferromagnetic order in the Mn layer. The band structures given in Fig. 3 (a) and (b) exhibit clearly the marked two-dimensional half metallic character of the heterostructure.

In order to better characterize the relevant conduction states, we examine the Fermi surfaces and associated charge density in Fig. 4. The band 1 forms a hole pocket, a surface with closed orbit, around the  $\Gamma$  point. Bands 2 and 3 form two electron surfaces centered at the R point in the  $\mathbf{k}_x$ - $\mathbf{k}_y$  plane. In Fig. 4(b), as an example for illustration, the corresponding majority-spin hole charge densities are obtained by integrating states in the vicinity of  $E_F$  up to 0.5 eV. It can be seen that the hole states are strongly confined in the vicinity of the Mn layer and distributed in the bonding directions between Mn and Si(I) atoms.

One important question is whether the half metallic character can be maintained up to  $T_C$  in this DFH. Based on an analysis of available experimental data on NiMnSb alloys, Hordequin *et al.* [23] identified the temperature  $T^*$  (80 K) well below  $T_C$  (730 K) at which NiMnSb undergoes an electronic phase transition from half metal to normal ferromagnet. This crossover occurs because the minority bandgap is the result of exchange splitting of bands, which is proportional to the magnetization and decreases as temperature increase. The interpretation is that one of the gap edges crosses the Fermi level as the gap decreases, thereby losing the half metal character. From Hall measurements, they found that the hole concentration increases with temperature and that the low  $T^*$  is the signature of spin flip transitions from the majority-spin states at  $E_F$  to the bottom of the conduction band of the minority-spin channel, which become allowed as the gap decreases. They concluded that  $T^*$  could reach  $T_C$  if  $E_F$  lies near the top of the valence band of the minority-spin channel, rather than near the bottom of the conduction band. Unlike NiMnSb, this advantageous band lineup does occur in the band structure of Mn/Si-DFH shown in Fig. 3. Fig. 3(c) shows a schematic diagram of density of states of Mn/Si-DFH near the  $E_F$ . The spin-flip gap  $\delta$  between the Fermi energy and the bottom of the conduction band in the minority-spin channel is about 0.16 eV, which is close to the semiconducting gap  $\Delta = 0.2$  eV from the

valence band maximum (VBM) to the bottom of the conduction band in the minority-spin channel. In addition, the bottom of the conduction band is well below the conduction band minimum (CBM) of host Si crystal. At finite temperature, there are two possible spin-flip transitions due to the interaction between the spin of a carrier and the fluctuation of local moments of the Mn atoms. One is the transition from the top of valence states in the minority-spin channel to the majority states at  $E_F$ , but this will be strongly suppressed by matrix element effects because the uppermost valence states are bulk Si bonding states whereas the states at  $E_F$  are Mn  $d$  - Si(I)  $p$  hybridized and they only weakly overlap bulk Si states. Thus, as in NiMnSb, only the second one dominates the spin-flip scattering and deteriorates the half metallicity, because both the majority states at  $E_F$  and the minority states at the bottom of conduction band are coming from the hybridized Mn  $d$  - Si  $p$  states. This second process, of an electron at the  $E_F$  undergoing a spin flip transition to the bottom of conduction band, involve the so-called spin-flip gap  $\delta$ . It should be mentioned that the GGA usually underestimate the semiconducting gap of Si crystal, and a wider gap  $\delta$  should be more realistic. Therefore, for the Mn/Si-DFH, the half metallic character could persist up to a temperature comparable to  $T_C$ .

In summary, using first-principles electronic-structure methods, we have designed a low strain DFH composed of a Mn  $\delta$ -doped layer in Si substrate, which exhibits two-dimensional half metallic properties. The metallic states are hybrid states originating from Mn- $t_{2g}$  and nearest-neighbor Si- $p$  states in the majority-spin channel. A semiconducting gap is retained between minority-spin bonding and antibonding states. From the DOS and band structure, the half metallic properties are shown to have marked two-dimensional character and are likely to persist up to  $T^* \approx T_C$ , in marked contrast to NiMnSb.

Since the measured  $T_C$  in dilutely doped Mn in bulk Si is approximately 400 K[17], the  $T_C$  for this ordered DFH may be substantially higher than room temperature. Due to the maturity of Si technologies, it may be expected that Si based devices will be more readily fabricated than their GaAs based counterparts. If the designed DFH can be grown, such Si based half metallic materials could lead to a breakthrough in the realization of spintronic devices in the near future, and to a new generation of devices in the years to come.

This work is partially supported by National Science Foundation with grant No. ESC-0225007, and the San Diego Supercomputer Center. This work was also performed, in part, under the auspices of the U. S. Department of Energy by the University of California,

- [1] Y. Ohno, D. K. Young, B. Beschoten, F. Matshkura, H. Ohno, and D. Awschalom, *Nature* **402**, 790 (1999).
- [2] G. A. Prinz, *Science* **282**, 1660 (1998).
- [3] P. Ball, *Nature* **404**, 918 (2000).
- [4] W. E. Pickett and J. S. Moodera, *Physics Today* **54**, 39 (2001).
- [5] H. Akinaga, T. Manago, and M. Shirai, *Jpn. J. Appl. Phys.* **39**, L1118 (2000).
- [6] J. H. Zhao, F. Matsukura, T. Takamura, E. Abe, D. Chiba, and H. Ohno, *Appl. Phys. Lett.* **79**, 2776 (2001).
- [7] J. E. Pask, L. H. Yang, C. Y. Fong, W. E. Pickett, and S. Dag, *Phys. Rev. B* **67**, 224420 (2003).
- [8] I. Galanakis and P. Mavropoulos, *Phys. Rev. B* **67**, 104417 (2003).
- [9] Wen-Hui Xie, Ya-Qiong Xu, and Bang-Gui Liu, D. G. Pettifor, *Phys. Rev. Lett.* **91**, 037204 (2003).
- [10] J. P. Perdew, K. Burke, and M. Ernzerhof, *Phys. Rev. Lett.* **77**, 3865 (1996).
- [11] C. Y. Fong, M. C. Qian, L. H. Yang, J. E. Pask, and S. Dag, *Appl. Phys. Lett.* **84**, 239 (2004).
- [12] C. Y. Fong and M. C. Qian, *J. Phys.: Condens. Matter* **16**, S5669 (2004).
- [13] M. C. Qian, C. Y. Fong, W. E. Pickett, J. E. Pask, L. H. Yang, and S. Dag, *Phys. Rev. B* **71**, 12414 (2005).
- [14] M. C. Qian, C. Y. Fong, W. E. Pickett, and Huai-Yu Wang, *J. Appl. Phys.* **95** 7459 (2004).
- [15] S. Sanvito and N. A. Hill, *Phys. Rev. Lett.* **87**, 267202 (2001).
- [16] Hongming Weng, Jinming Dong, *Phys. Rev. B* **71**, 035201 (2005).
- [17] M. Bolduc, C. Awo-Affouda, A. Stollenwerk, M. B. Huang, F. G. Ramos, G. Agnello, and V. P. LaBella, *Phys. Rev. B* **71**, 033302 (2005).
- [18] F. M. Zhang, X. C. Liu, J. Gao, X. S. Wu, Y. W. Du, H. Zhu, J. Q. Xiao, and P. Chen, *Appl. Phys. Lett.* **85**, 786 (2004).
- [19] G. Kresse and J. Hafner, *J. Phys.: Condens. Matter* **6**, 8245 (1994); G. Kresse and J. Furthmuller, *Phys. Rev. B* **54**, 11169 (1996).
- [20] D. Vanderbilt, *Phys. Rev. B* **41**, R7892 (1990).

- [21] M. C. Qian *et al.* (unpublished).
- [22] H. J. Monkhorst and J. D. Pack, Phys. Rev. B **13**, 5188 (1976).
- [23] C. Hordequin, D. Ristoiu, L. Ranno, and J. Pierre, Eur. Phys. J. B **16**, 287 (2000).

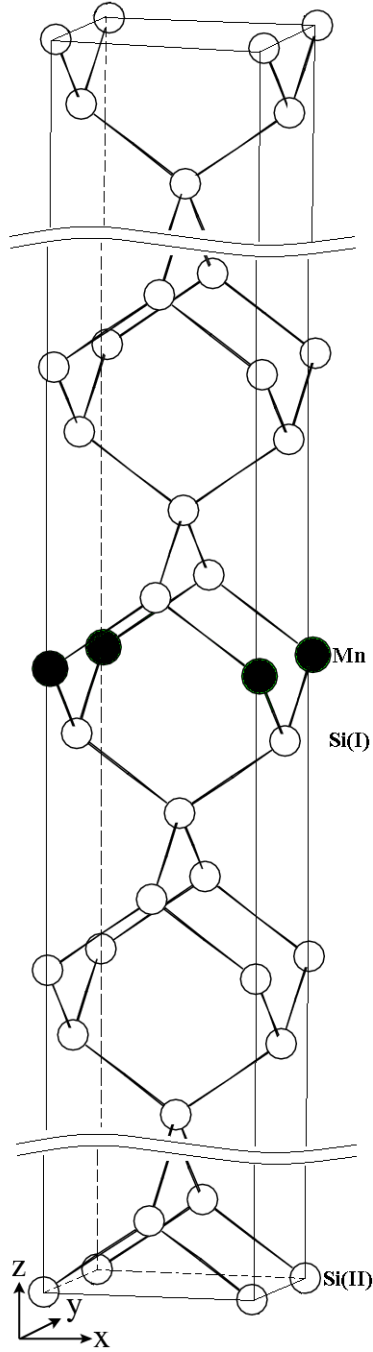


FIG. 1: Mn/Si-DFH unit cell, consisting of 32 layers in the z-direction. Black circles denote Mn; open circles denote Si.

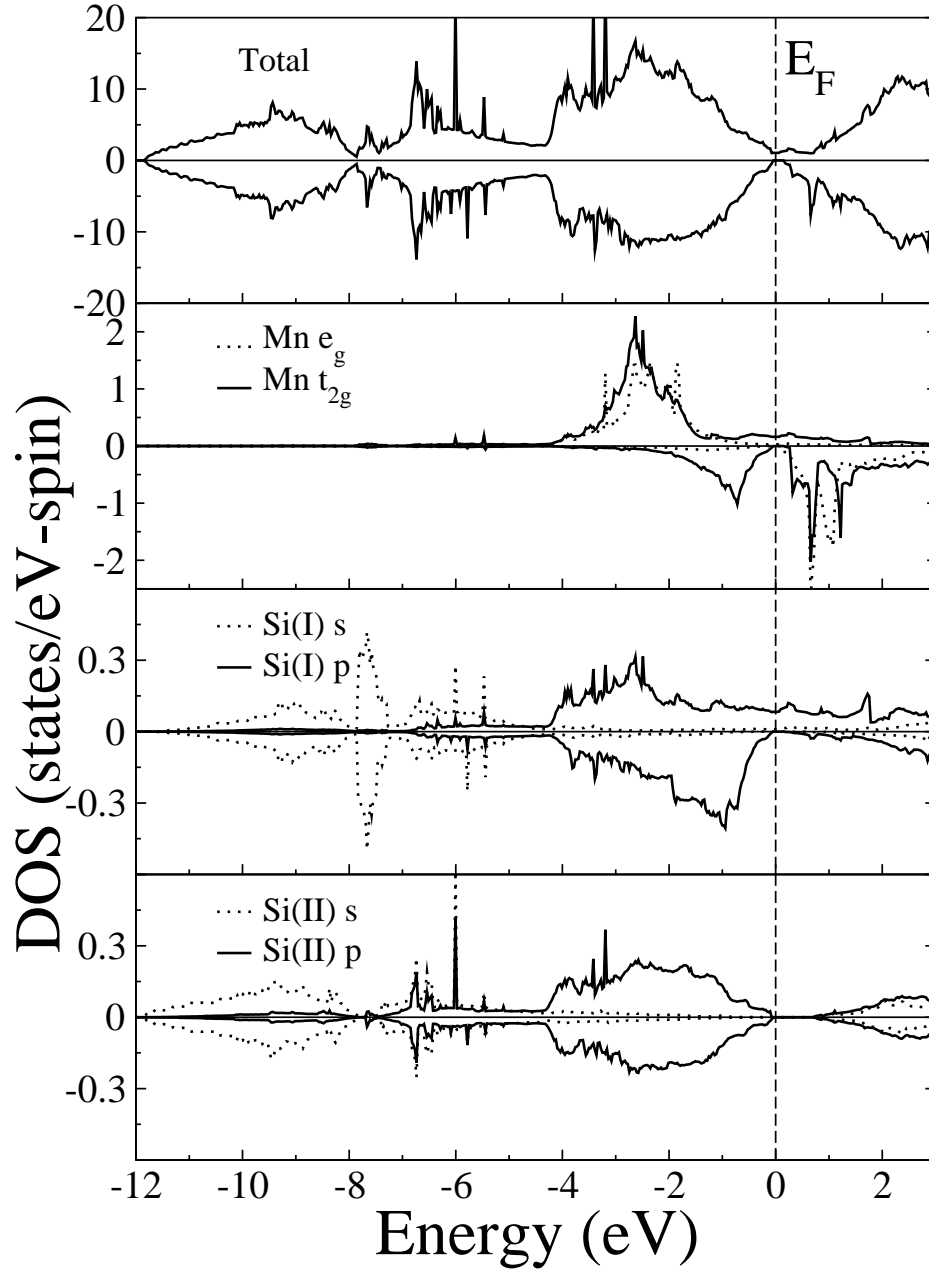


FIG. 2: Calculated total and partial densities of states for Mn  $\delta$ -doped in Si. Si(I) and Si(II) refer to nearest and farthest silicons from Mn. Majority densities are plotted as positive values; minority densities, as negative. The vertical dashed line indicates the Fermi energy.

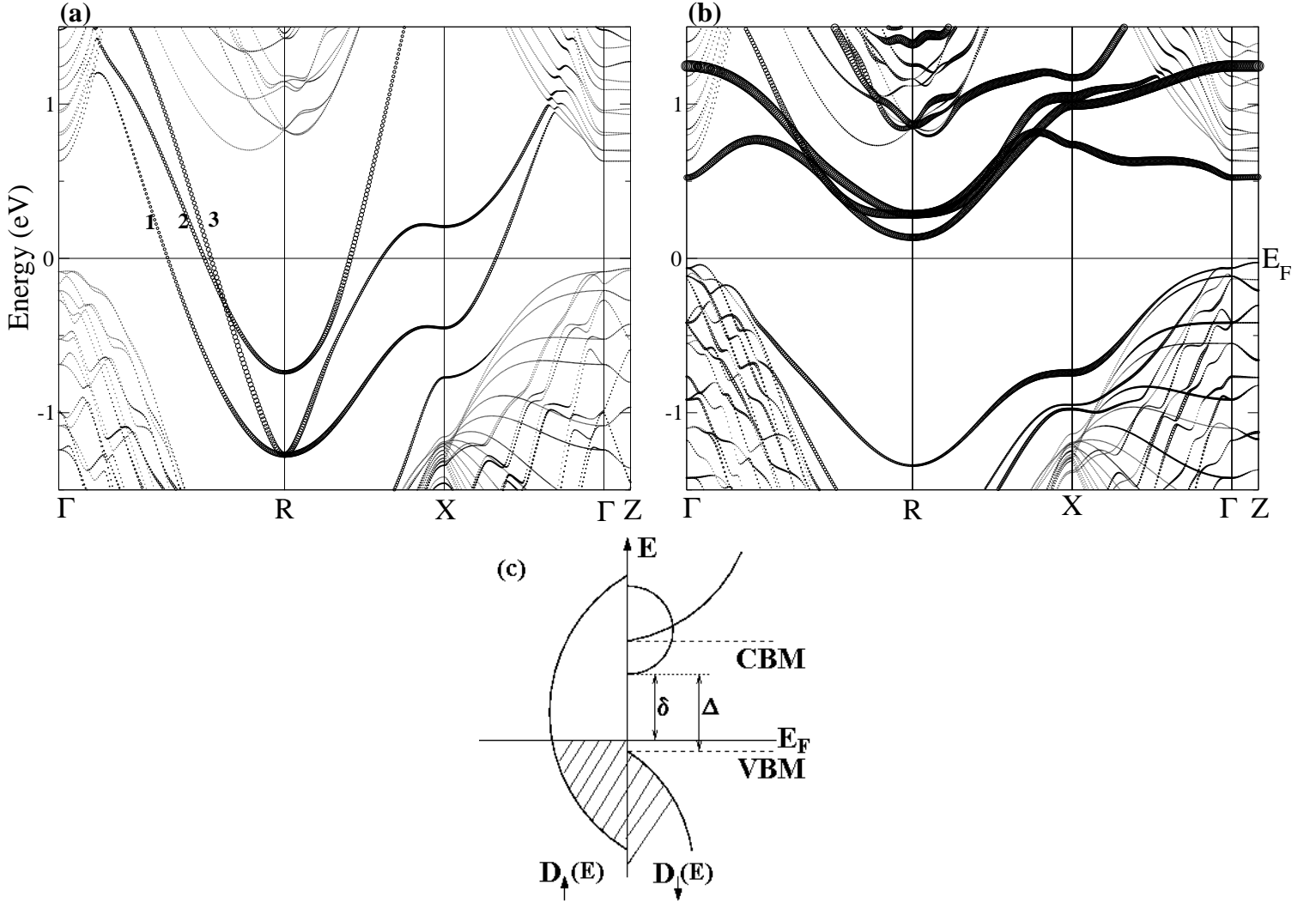


FIG. 3: Calculated band structure along  $\Gamma$ -R-X- $\Gamma$  in the  $k_x$ - $k_y$  plane and along  $\Gamma$ -Z in the  $k_z$ -direction, (a) spin up and (b) spin down for Mn  $\delta$ -doped in Si. High symmetry points of the Brillouin zone are  $\Gamma = (0, 0, 0)$ , R=  $(1, 1, 0)$ , X=  $(1, 0, 0)$ , and Z=  $(0, 0, 1)$ . The size of circles indicates the fraction of Mn  $d$  character. The conduction bands are labeled 1, 2 and 3. (c) Schematic diagram of the density of states  $D(E)$  in Mn/Si-DFH of the two spin channels near  $E_F$ . VBM and CBM are the valence band maximum and conduction band minimum, respectively, of Si crystal for comparison.

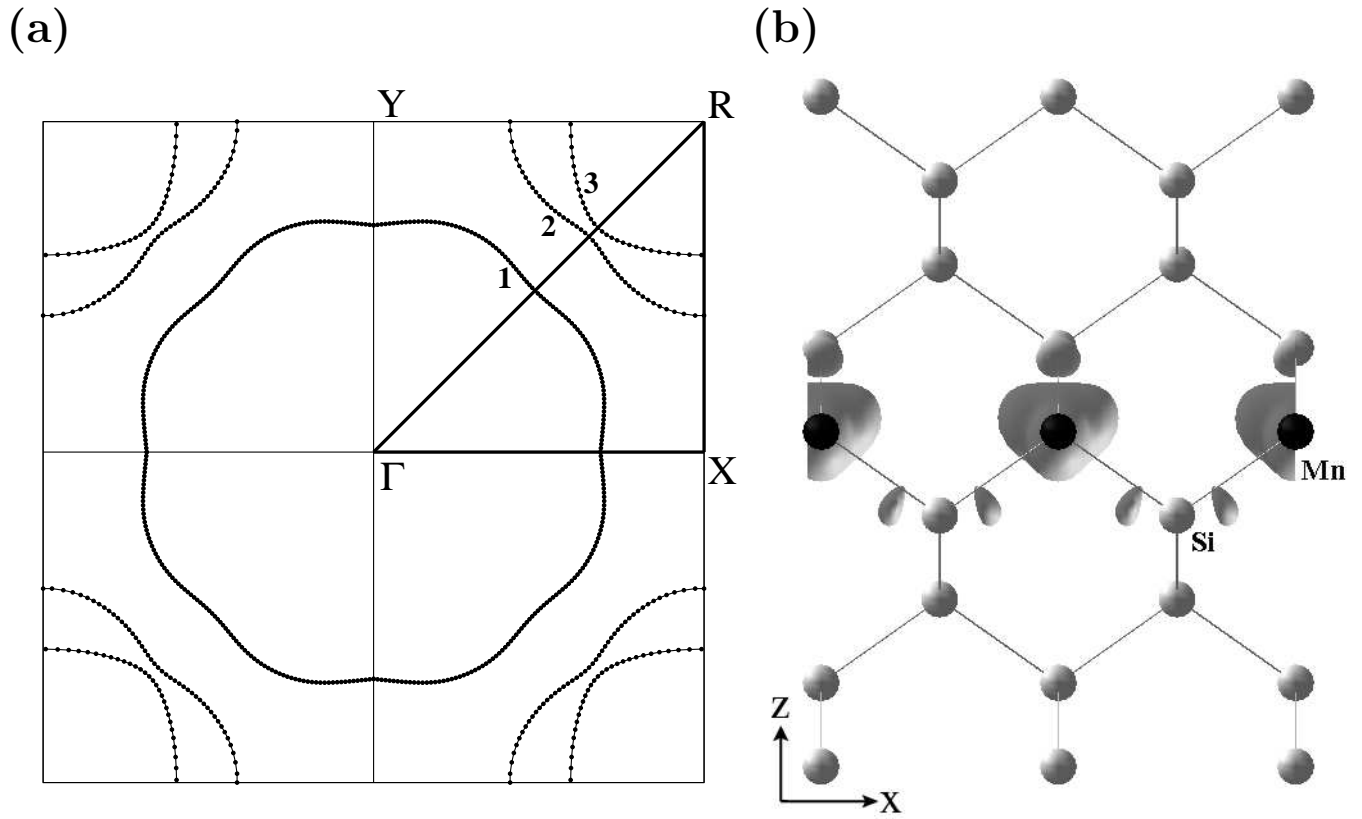


FIG. 4: (a) Calculated two-dimensional Fermi surfaces. (b) Majority-spin hole charge density in the vicinity of  $E_F$  for Mn  $\delta$ -doped in Si.